Computer simulation of internal combustion engine flow processes

C.M. van Vuuren[1] G.D. Thiart[2] A.B. Taylor[3]

(First received January 2002; Final version May 2002)

A computer code for the simulation of internal combustion engine processes is presented. The main objective of the code is to serve as a tool for the design of inlet and outlet manifolds of combustion engines. The code is built around a two-zone thermodynamic combustion model that is linked to a quasi one-dimensional unsteady method of characteristics pipe flow model and a camshaft model. Two simple test cases are presented to show that the pipe flow model functions correctly. Predictions of the crankshaft power delivered by a commercial internal combustion engine computed by means of the code are shown to compare favourably with measured results. An example illustrating the usefulness of the code as a design tool is also presented.

Nomenclature

A	pipe cross-sectional area
c	speed of sound
c_p	specific heat at constant pressure
D	hydraulic diameter
f	fanning pipe friction factor
h	coefficient of heat transfer
p	static pressure
R	ideal gas constant
Re	Reynolds number ($= \rho u D/\mu$)
T	temperature
u	velocity
γ	ratio of specific heats
μ	dynamic viscosity
ρ	density

Subscripts

g	gas in pipe
t	partial differentiation w.r.t. time
w	pipe wall
x	partial differentiation w.r.t. distance

Introduction

The cycle of operations within a cylinder of a conventional four-stroke internal combustion engine (ICE) can be subdivided into the gas exchange process, where the products of combustion are exhausted and replaced by a fresh air/fuel mixture, and the power process, where the air/fuel mixture is compressed, ignited and the hot gas expanded to produce useful work. The gas exchange process is caused primarily by the pumping action of the piston, but there are usually also interactions with the intake and exhaust systems that affect the efficiency of the gas exchange process.

The correct sizing of the length and diameter of inlet manifolds is particularly important in achieving optimum performance — peaks in volumetric efficiency of an engine occur when the natural frequency of the intake system is "in tune" with the engine induction period, so that the pressure at the inlet valve is raised in the critical region around bottom dead centre of the induction stroke, before the valve closes. Benson[1] and others (e.g. Stone & Etiman[2]) found that variations in inlet manifold length not only affect the engine speed at which the engine performs at its optimum, but can also increase the maximum torque produced by the engine.

Attempts to simulate ICE processes date back to at least the 1950s; software codes for ICE simulation employ various models to simulate these processes, from simple empirical based theory, through one-dimensional models, to fully three-dimensional computational fluid dynamic (CFD) models. Each step in this progression requires a vast increase in computer power, the fully three-dimensional CFD codes such as PowerFLOW[3] requiring powerful workstations for even the simplest cases.

One-dimensional thermodynamic models for in-cylinder pressure and temperature calculations (see, for example, Benson[1]) are reasonably simple and have been used in personal computer (PC) based models, e.g. SPICE II[4] and DYNOMATION[5] for many years. Often these codes make use of very simple in-cylinder and wave action models to predict engine performance for a given set of operating conditions. These simplifications are made in order to reduce processing time, e.g. to produce a simple torque *vs* engine speed curve within a few minutes. Recent advances in PC technology have, however, lead to the possibility of developing codes for the PC, which can simulate the complex unsteady pulsed flows in ICE manifolds. The purpose of this paper is to describe such an ICE simulation code that has been developed at the University of Stellenbosch.

Overview of the engine simulation code

The code called ESA (Engine Simulation and Analysis) was written in Pascal in the object oriented 32 bit Borland Delphi environment, and is compiled as a Microsoft Windows application. It consists of the two-zone thermodynamic combustion model, developed by Williams,[6] linked to a quasi one-dimensional unsteady method of character-

1. MScEng student, Department of Mechanical Engineering, University of Stellenbosch

2. Associate Professor, Department of Mechanical Engineering, University of Stellenbosch

3. Senior Lecturer, Department of Mechanical Engineering, University of Stellenbosch, Private Bag X1, Matieland, 7602 South Africa

istics (MOC) manifold and pipe flow model, developed by Van Vuuren,[7] and is integrated with a camshaft model, also developed by Williams.[6] The MOC, such as described by Shapiro[8] or Zucrow & Hoffman,[9] is a mature tool for the analysis of quasi one-dimensional (i.e. one-dimensional flow through variable cross-section ducts) unsteady flow, and the details will therefore not be presented here. A summary of the governing equations are given in the Appendix.

The computational domain extends from the plenum end of the inlet tract, through the manifold tract, inlet valves, cylinder, exhaust valves, and exhaust tract up to the first expansion of the exhaust at a silencer box. It incorporates modelling of one cylinder only; no interaction between cylinders in the form of pressure pulses are accounted for. The code computes simultaneous solutions of the governing equations of all the sub-models at time steps corresponding to 1° increments throughout the 720° of crankshaft revolution (four-stroke operation is assumed), i.e.

- solution of the equations of state to obtain the gas properties inside the cylinder;
- computation of the pressure, temperature and velocity distributions inside the inlet and exhaust tracts by means of the MOC;
- calculation of the mass flow through the valves, based on the pressure difference across the valve, the valve lift and the valve discharge coefficient; and
- a mass and energy balance inside the cylinder, with heat addition where there is combustion, and losses where there is heat transfer and friction.

This procedure is repeated until a "steady-state" solution is obtained. Usually 5–10 cycles are sufficient for convergence. Results such as in-cylinder gas properties, the pressure-volume diagram, etc. are displayed graphically, and updated continuously throughout a simulation. We will not present any central processor unit (CPU) time data for the running of simulations here. Suffice it to say that the biggest limitation on the running speed of the ESA software is not the speed of the CPU, but the speed of the graphics card.

Verification of the pipe flow model

The verification of the pipe flow model was done by comparing computational results with the experimental measurements reported by Kirkpatrick *et al.*[10] Their experimental rig consisted of a single cycle pressure wave generator consisting of a thermally insulated cylinder connected to a 5 901 mm long pipe via a sliding valve, the other end of the pipe being open to atmosphere. The pressure waves created by this rig reportedly imitate those to be found in the inlet and exhaust systems of ICEs closely. Static pressure and temperature were recorded by transducers positioned on the cylinder and at various locations along the pipe. In the two case studies that follow, the pressures recorded at the cylinder, and at positions 317 mm and 3 691 mm (hereafter referred to as "station 1" and "station 2", respectively) downstream of the cylinder, are compared with those computed by meams of the ESA pipe flow model.

Case study 1: Simulation of an induction process

In this experiment, the gas in the cylinder is at a pressure lower than atmosheric, which is 1 bar. The valve is opened linearly (w.r.t. time) to full pipe bore and then closed again. Computational values of pressure are compared with the corresponding measured ones in Figures 1–3, for the case where the air inside the cylinder was at 0.5 bar and 293 K initially. The correspondence between measured and computed values is generally good. It is especially gratifying that the final pressure in the cylinder is captured correctly, as is evident in Fig. 1.

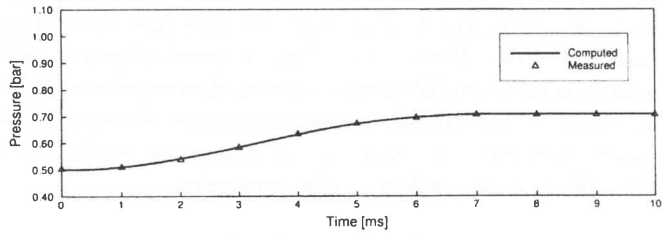


Fig. 1. Induction process pressure traces at cylinder

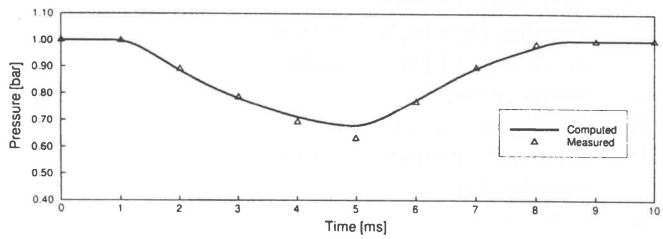


Fig. 2. Induction process pressure traces at station 1

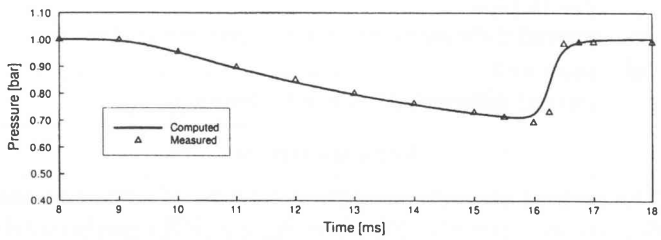


Fig. 3. Induction process pressure traces at station 2

Case study 2: Simulation of an exhaust process

Here the gas in the cylinder is at a pressure higher than atmosheric pressure, which is again 1 bar. The valve is again opened linearly to full pipe bore and then closed again. Computational values of pressure are compared with the corresponding measured ones in Figures 4–6, for the case

where the air inside the cylinder was at 1.5 bar and 293 K initially. Again the correspondence between measured and computed values is generally good, and again the final pressure in the cylinder is captured correctly as shown in Fig. 4.

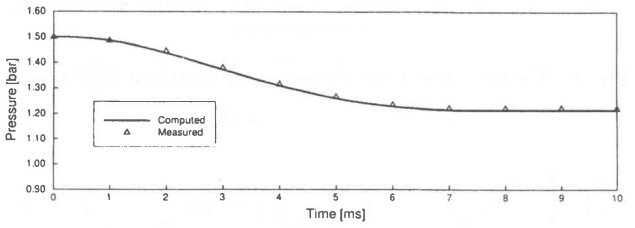


Fig. 4. Exhaust process pressure traces at cylinder

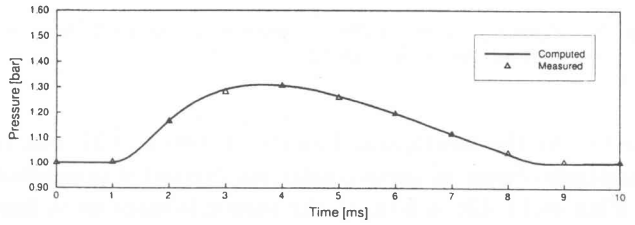


Fig. 5. Exhaust process pressure traces at station 1

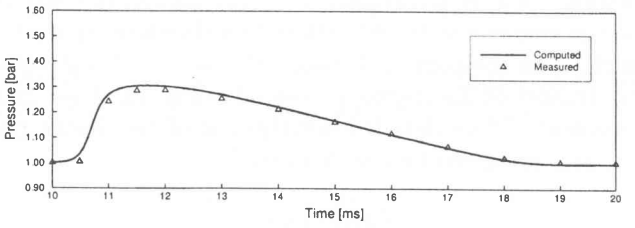


Fig. 6. Exhaust process pressure traces at station 2

Comparison with engine test data

In order to verify that the ESA code predicts the correct trends (e.g. decrease or increase in power) when any particular engine parameter is varied, and to quantify the accuracy of these predictions, a number of experiments were performed using a commercial four cylinder 8-valve, overhead cam, 2.4 ℓ cross-flow fuel-injected engine. Its inlet and exhaust systems were modified so that one cylinder could be isolated, i.e. its inlet and exhaust pipes could be isolated from the inlet and exhaust manifolds, respectively. The engine was mounted on a test bench that facilitated the recording of brake torque, as well as other data that are not relevant here. Also, high-speed DYTRAN pressure sensors were used to measure the pressure trace at various points along the inlet pipe of one cylinder, and at the inlet manifold.

TABLE I
Measured vs predicted power as function of engine speed and inlet length

Engine speed [r.p.m.]	Inlet length [mm]	Measured power [kW]	Predicted power [kW]	Difference [%]
2000	290	40.0	39.9	−0.3
	390	41.3	40.5	−1.9
	490	42.0	40.9	−2.6
3000	290	58.1	59.0	1.5
	390	60.4	60.4	0.0
	490	62.7	62.9	0.3
4000	290	69.6	71.6	2.9
	390	72.7	71.7	−1.4
	490	71.8	70.3	−2.1
5000	290	68.2	73.2	7.3
	390	68.7	70.2	2.2
	490	63.6	65.5	3.0

The first set of tests was performed with all four cylinders connected to the inlet and exhaust manifolds. The length of the inlet pipes was increased in steps of 100 mm, from 290 mm total length to 490 mm total length. Experimental results and those predicted by the ESA code are compared in Table I. It is clear that the model predicts the engine power reasonably well, with a maximum difference of approximately 7% at 5 000 r.p.m. The measured and predicted trends, regarding the increase in power for a 200 mm change in inlet length, are compared in Table II, from which it is evident that the predicted trend lags the measured trend by 3 to 5 percentage points.

A second series of tests was run with one of the cylinders isolated from the remaining three, as explained before. Measured pressure traces at the cylinder head (10 mm from the head face) are compared in Figs. 7–9 with those predicted by the ESA code, for the three different inlet lengths, at 4 000 r.p.m. Note that the inlet valve opens at 340° and closes at 580°, whilst the exhaust valve opens at 120° and closes at 390°. It is evident from these figures that the ESA code predicts the frequency of the pressure pulses correctly, but that it generally overpredicts the amplitudes, especially at higher engine speeds.

TABLE II
Measured vs predicted power for a 200 mm increase in inlet length

Engine speed [r.p.m.]	Measured power increase [%]	Predicted power increase [%]
2000	5.0	2.5
3000	7.9	6.6
4000	3.2	−1.8
5000	−6.7	−10.5

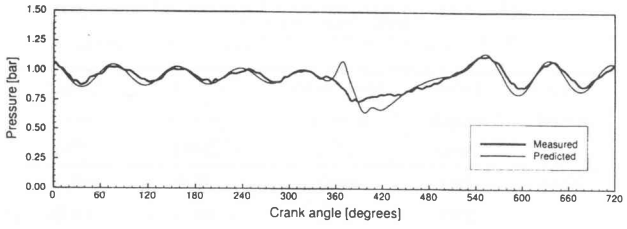


Fig. 7. Pressure traces for 290 mm inlet length at 4000 r.p.m.

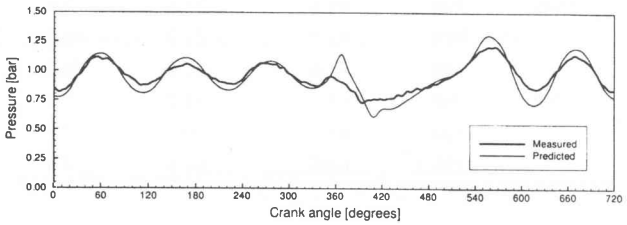


Fig. 8. Pressure traces for 390 mm inlet length at 4000 r.p.m.

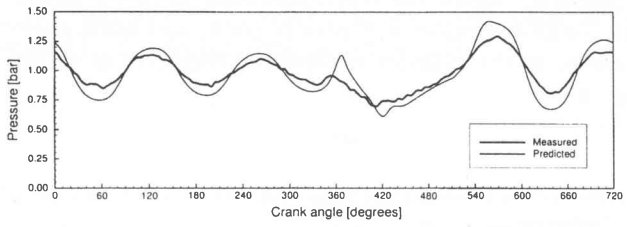


Fig. 9. Pressure traces for 490 mm inlet length at 4000 r.p.m.

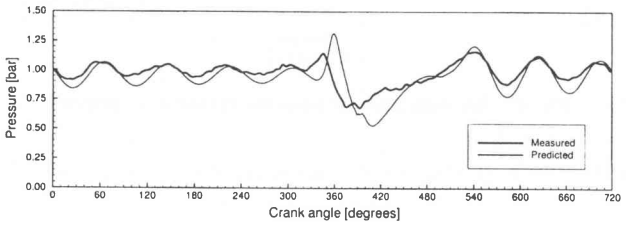


Fig. 10. Pressure traces for 290 mm inlet length at 4000 r.p.m. and camshaft advanced through 12°

A third series of tests was run, with the 290 mm length inlet, but with the camshaft advanced through 12° relative to the setting for the first and second series of tests. Experimental results and those predicted by the ESA code are compared in Table III, from which it is again evident that the model predicts the engine power reasonably well. The measured and predicted trends regarding the increase in power for a 12° change in camshaft angle corresponds reasonably well, especially at higher engine speeds, as shown in Table IV. Pressure traces for an engine speed of 4 000 r.p.m. are compared in Fig. 10.

TABLE III

MEASURED VS PREDICTED POWER FOR AN INLET LENGTH OF 290 MM AND CAMSHAFT ADVANCED THROUGH 12°

Engine speed [r.p.m.]	Measured power [kW]	Predicted power [kW]	Difference [%]
2000	40.0	39.1	−2.3
3000	57.8	55.7	−3.6
4000	62.7	63.1	0.6
5000	56.9	57.0	0.2

UTILIZATION OF THE ESA SOFTWARE AS A DESIGN TOOL

The ESA software has already been employed in several engine upgrade projects where an increase in performance of an existing engine was required. One such example is that of a four cylinder 1.6 ℓ 20 valve engine, of which it was required to develop its maximum torque of 150 Nm at or close to 4 000 r.p.m., and its maximum power of 78 kW at approximately 6 000 r.p.m. The ESA software was used to compute the torque delivered by the engine as function of inlet manifold length and diameter, and the results were used to fix the length and diameter at 686 and 37 mm, respectively. Some of these results are presented graphically in Figures 11–12: in Fig. 11 the torque is mapped as function of engine speed and manifold length for a manifold diameter of 37 mm, and in Fig. 12 the torque is mapped as function of manifold diameter for a manifold length of 686 mm.

A prototype manifold was subsequently designed and manufactured in accordance with the quoted dimensions, and the engine was tested with it on a standard engine test bench. The comparison between the predicted and tested performance of the engine, presented in Fig. 13, shows good agreement. More detailed descriptions of the design process, etc. are given by Van Vuuren.[7]

CONCLUSION

From the results presented in this paper, it is evident that the ESA code is capable of simulating ICE processes realistically. The code has also been used successfully in the design of manifold systems for a local engine manufacturer, as illustrated by the example in the foregoing section.

TABLE IV

MEASURED VS PREDICTED POWER FOR AN INLET LENGTH OF 290 MM AND A DIFFERENCE OF 12°IN CAMSHAFT ANGLE

Engine speed [r.p.m.]	Measured power increase [%]	Predicted power increase [%]
2000	5.0	2.5
3000	7.9	6.6
4000	3.2	−1.8
5000	−6.7	−10.5

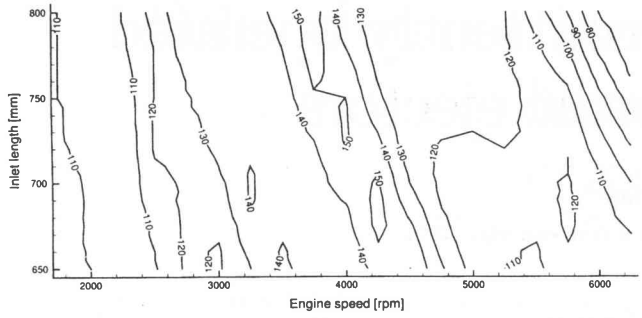


Fig. 11. Torque contours for an inlet manifold diameter of 37 mm

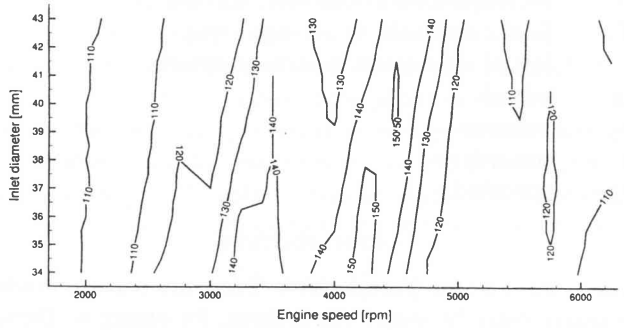


Fig. 12. Torque contours for an inlet manifold diameter of 686 mm

Notwithstanding its achievements, the code still has a number of shortcomings for which further research and development are required. Useful extensions to the code would be the capability to simulate multi-cylinder engine processes and simulation of turbo-charged engines.

References

[1] Benson RS. *The Thermodynamics and Gas Dynamics of Internal Combustion Engines: Vol. 1.* Clarendon Press, Oxford, 1982.

[2] Stone CR & Etiman Y. Review of induction system design and a comparison between prediction and results from a single cylinder diesel engine. *SAE paper No. 921734*, 1992.

[3] Molvig K. *PowerFLOW.* Exa Corporation, Lexington, 1991.

[4] Charlton SJ. *Simulation program for internal combustion engines.* University of Bath, 1990.

[5] *DYNOMATION — Four Cycle Wave Action Simulator.* Audie Technology Inc. and VP Engineering Inc., 1994.

[6] Williams PNT. Modelling of internal combustion engine thermodynamics, valve dynamics and valve flow. MScEng thesis, University of Stellenbosch, 2002.

[7] Van Vuuren CM. Modelling of internal combustion engine intake and exhaust processes. MScEng thesis, University of Stellenbosch, 2001.

[8] Shapiro AH. *The Dynamics and Thermodynamics of Compressible Fluid Flow: Vol. II.* Ronald Press, 1954.

[9] Zucrow MJ & Hoffman JD. *Gas Dynamics: Vol. II.* Wiley, New York, 1976.

[10] Kirkpatrick SJ, Blair GP, Fleck R & McMullen RK. Experimental evaluation of 1-D computer codes for the simulation of unsteady gas flow through engines — a first phase. *SAE paper No. 941685*, 1994.

[11] Kays WM & Crawford ME. *Convective Heat and Mass Transfer.* McGraw-Hill, New York, 1993.

[12] Holman JP. *Heat Transfer.* McGraw-Hill, New York, 1992.

[13] Low SC & Baruah PC. A generalized computer aided design package for I.C. engine manifold systems. *SAE paper No. 810498*, 1981.

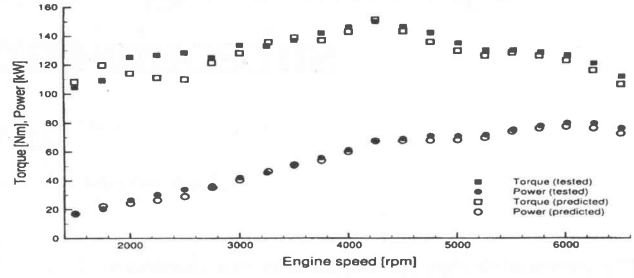


Fig. 13. Comparison between predicted and test data for the 1.6 *l* engine upgrade

Appendix

The governing equations for the pipe flow model are those of non-homentropic flow, which implies that there can be friction in the system, as well as heat transfer to the system. They are as follows for an ideal gas with constant heat capacity:[1,9]

- Conservation of mass

$$\rho_t + u\rho_x + \rho u_x + \frac{\rho \mathrm{A}_x}{A} = 0 \tag{A.1}$$

- Conservation of momentum

$$u_t + \mathrm{u}_x + \frac{p_x}{\rho} + \frac{u\,|u|}{2} \cdot \frac{4f}{D} = 0 \tag{A.2}$$

- Conservation of energy

$$\begin{aligned} &p_t + up_x - c^2\left(\rho_t + u\rho_x\right) \\ &= \rho(\gamma - 1)\left[\frac{\pi Dh}{\rho A}\left(T_w - T_g\right) + \frac{u^2\,|u|}{2} \cdot \frac{4f}{D}\right] \end{aligned} \tag{A.3}$$

- Equation of state

$$p = \rho RT \tag{A.4}$$

- The speed of sound is given by

$$c^2 = \frac{\gamma p}{\rho} \tag{A.5}$$

- The Fanning friction factor is modelled as a function of the instantaneous Reynolds number:[9,11,12]

$$f = \begin{cases} 16/\,\mathrm{Re} & \text{for laminar flow } (\mathrm{Re} < 2300) \\ 0.0791/\,\mathrm{Re}^{0.25} & \text{for transitional flow } (2300 \le \mathrm{Re} \le 4000) \\ 0.04/\,\mathrm{Re}^{0.16} & \text{for turbulent flow } (\mathrm{Re} > 4000) \end{cases} \tag{A.6}$$

- The convective heat transfer coefficient is also modelled as a function of Reynolds number

$$h\left[\mathrm{W/m^2 \cdot K}\right] = \begin{cases} 10 & \text{for laminar flow } (\mathrm{Re} < 2300) \\ \frac{1}{2}\rho u f c_p & \text{for transitional and turbulent flow } (\mathrm{Re} > 2300) \end{cases} \tag{A.7}$$

Note the underlying assumption that friction and heat transfer under unsteady conditions are the same as for steady conditions.